Clinical Neurology and Neuroscience
2021; 5(4): 82-97
http://www.sciencepublishinggroup.com/j/cnn
doi: 10.11648/j.cnn.20210504.13
ISSN: 2578-8922 (Print); ISSN: 2578-8930 (Online)

The NRF1/miR-4514/SOCS3 Pathway Is Associated with Schizophrenia Pathogenesis

Yilin Liu†, Shujun Li†, Xiao Ma, Qing Long, Lei Yu, Yatang Chen, Wenzhi Wu, Zhichao Guo, Zhaowei Teng, Yong Zeng*

The Sixth Affiliated Hospital of Kunming Medical University, Yuxi, China

Email address:

zengyong@kmmu.edu.cn (Yong Zeng)

*Corresponding author

† Yilin Liu and Shujun Li are co-first authors.

To cite this article:

Yilin Liu, Shujun Li, Xiao Ma, Qing Long, Lei Yu, Yatang Chen, Wenzhi Wu, Zhichao Guo, Zhaowei Teng, Yong Zeng. The NRF1/miR-4514/SOCS3 Pathway Is Associated with Schizophrenia Pathogenesis. *Clinical Neurology and Neuroscience*. Vol. 5, No. 4, 2021, pp. 82-97. doi: 10.11648/j.cnn.20210504.13

Received: September 27, 2021; **Accepted**: October 15, 2021; **Published**: October 28, 2021

Abstract: *Background:* Schizophrenia (SZ) is a common and severe mental disease. However, its etiology and pathogenesis have not been fully established. In this study, bioinformatics was used to identify SZ-related genes and reveal the potential mechanisms of them. *Methods:* Gene expression profiles were obtained from the GSE46509 dataset. Differentially expressed genes (DEGs) were analyzed by Gene Ontology (GO) and the Kyoto Encyclopedia of Genes and Genomes (KEGG) pathway enrichment databases. A protein-protein interaction (PPI) network was established. TargetScan and miRGen, which are based on bioinformatics algorithms, were used to predict potential candidate target miRNAs and transcription factors. *Results:* Compared to healthy people controls, a total of 1422 DEGs were identified in SZ patient samples. Functional enrichment analysis revealed that these DEGs were significantly enriched in RNA processing, mRNA binding, and cell adhesion molecules. In addition, in the PPI network, SOCS3, FBXO9, ASB17, FBXO10, and ASB4 were identified as hub genes. In the predicted TF-miRNA-mRNA targeting regulatory network, hsa-miR-4514 was up-regulated by the highly expressed transcription factor (TF) NRF1, which down-regulated multiple hubs genes such as SOCS3, FBXO9, and FBXO10. *Conclusions:* Several potential biomarkers involved in SZ development were identified by bioinformatics analyses. Furthermore, our findings revealed the underpinning mechanisms of these potential biomarkers in the pathogenesis of SZ. And these results suggest a potential application value in clinical practice.

Keywords: Schizophrenia, Bioinformatics, Regulatory Network, MicroRNAs, Transcription Factors

1. Introduction

Approximately 1% of the world's population with a diagnosis with schizophrenia (SZ). Globally, this disease is one of the top 10 causes of disability, and it accounts for 1.7% of the total global disease burden [1]. Currently, the criteria of schizophrenia are based on clinical history, symptoms, and behaviors. These include positive symptoms such as thought disorders, hallucinations, and delusions, as well as negative symptoms such as social withdrawal, unconsciousness, and poverty of thought. Moreover, there is a range of cognitive abnormalities, particularly attention, memory, and executive functioning deficits [2]. Appropriate diagnostic and treatment biomarkers have not been established. Therefore, elucidation of the etiology and molecular pathogenesis of schizophrenia will improve diagnostic rates and treatment outcomes.

Schizophrenia is a complex polygenic genetic disorder that is associated with multiple environmental factors. The roles of genetic factors and immune transmitters in SZ development have been documented [3, 4]. Multiple mechanisms are involved in regulation of gene expression. Non-coding RNA, a typical example of these mechanisms. It is associated with disease pathogenesis and progression [5]. MicroRNAs (miRNAs) constitute a class of small non-coding RNA molecules whose function is to specifically bind untranslated regions of target transcripts. Many miRNAs and their downstream target genes have been reported to be associated with SZ development [6, 7]. Serum [8] and peripheral blood monocyte [9] miRNAs are important diagnostic biomarkers of schizophrenia. Besides,

bioinformatic predictions and experimental validation, found that miRNAs can directly combine with target mRNA 3′untranslated region (3′-UTR), to perform its translational inhibition [5]. Transcription factors (TFs) regulate transcriptional initiation by binding promoter regions of the target genes, providing a switch for gene expression. Transcription factors regulate miRNA genes in the same way they, by combining with the binding site in, or near, promoter regions of miRNA precursors (pre-miRNA) [10, 11]. Coexpression networks driven by combinatorial and interactive actions from TFs and miRNAs are associated with SZ [12]. However, few studies have focused on the role of integrated regulation network of TFs-miRNAs-mRNA in SZ pathogenesis.

In this study, we selected the original microarray dataset from the Gene Expression Omnibus (GEO) databases. Bioinformatics methods were utilized to identify differentially expressed genes (DEGs). followed by Gene Ontology (GO) functional annotation analysis， Kyoto Encyclopedia of Genes and Genomes (KEGG) pathway enrichment analysis, and protein-protein interaction (PPI) analysis. Finally, the hub genes were screened for further analysis and predicting their related miRNAs and transcription factors. We constructed a TFs-miRNAs-mRNAs regulatory network and explored the molecular mechanisms associated with SZ pathogenesis.

2. Materials and Methods

2.1. Access to GEO Datasets

The Gene Expression Omnibus (GEO, http://www.ncbi.nlm.nih.gov/geo) is a public functional genomics data repository of high throughout gene expression data, chips, and microarrays. We selected the potential GEO datasets according to the following inclusion criteria: Schizophrenia and Homo sapiens. One microarray dataset generated from the superior frontal nerve cells of patients with SZ and controls was used in the study. The GSE46509 dataset is based on the GPL1352 platform ([U133_X3P] Affymetrix Human X3P Arrayincludes) with 8 SCZ patients and 8 normal controls. The data used in this paper are freely available online. Since this study was not performed in humans or animals, ethical approval was waived.

2.2. Data Analysis and Differential Expressions

An R-based online tool, GEO2R (http://www.ncbi.nlm.nih.gov/geo/geo2r), was used for the analysis of differentially expressed genes (DEGs). Data were retrieved from the GEO database and analyzed using GEO2R. There were no recognizable gene symbols and gene identifiers with a gene symbol greater than 1 were deleted. $p \leq 0.05$ and |log2 fold change (FC)| greater than 1 were considered to statistically significant. In addition, the volcano plotting tool (http://sangerbox.com/Tool) and TBtools softwares (https://github.com/CJ-Chen/TBtools) were used to visualize the volcano and heat maps of DEGs, respectively [13].

2.3. GO and KEGG Pathway Enrichment Analyses

GO function annotations and KEGG pathway enrichment analyses of the DEGs were performed using the online analysis tool, Visualization and Integrated Discovery (DAVID version 6.8, https://david.ncifcrf.gov/). This database includes basic data and analytical tools to provide a wide-scale gene or protein database and includes a comprehensive assessment of biological functions [14]. When screening important GO terms and KEGG pathways, $p < 0.05$ indicated that there were statistically significant differences. Two online sites (http://www.ehbio.com/Cloud_Platform/front/ and http://sangerbox.com/Tool) were used to display the results.

2.4. PPI Network Construction and Analysis

Based on laboratory data, high-throughput text mining, and predictive bioinformatics data, The STRING (Search Tool for the Retrieval of Interacting Genes/Proteins, https://string-db.org/) online database was used to evaluate interactions between candidate proteins [15]. Analysis of functional interactions between proteins can provide insights into the mechanisms of disease onset or progression. The STRING database was used to construct a PPI network, and the retrieved result was visualized using Cytoscape (an open-source bioinformatics software platform, version 3.8.2). Molecular Complex Detection (MCODE), a plugin in Cytoscape, is an application for clustering a given network based on topology to discover densely connected regions [16], was used to screen modules of the PPI network. Subsequently, GO terms and KEGG pathway enrichment analyses of DEGs in the key module were performed using the ClueGO and CluePedia plugin [17, 18]. Moreover, hub proteins or genes were obtained using the CytoHubba plugin of Cytoscape [19].

2.5. Prediction of Target miRNA and Construction of the TF-miRNA-mRNA Regulatory Network

Hub genes were defined as the genes that play essential roles in the network, according to the cut-off criteria calculated by CytoHubba. The topological analysis method, MCC (Maximal Clique Centrality), provided by CytoHubba was used to sequence and evaluate the Hub genes. The TargetScan database (http://www.targetscan.org/vert_71/) is an online database for miRNA prediction and functional annotations [20]. To investigate the regulatory mechanisms of the biomarkers, an miRNA targeting the hub genes was predicted with an online miRNA prediction tool of TargetScan. The Venn diagram (http://bioinformatics.psb.ugent.be/webtools/Venn/) was used to identify target miRNAs, and the overlapped target miRNAs were added for further analysis. Then, regulatory networks of the miRNA-mRNA pairs were extracted and visualized using the Cytoscape software. The potential transcription factors upstream of miRNA were predicted using DIANA-miRGen v3.0 [21]. Finally, the TF-miRNA-mRNA interaction network was constructed and visualized using Cytoscape.

3. Results

3.1. Identification and Analysis of DEGs in the GEO Dataset

The gene expression GSE46509 dataset was retrieved from the GEO database and analyzed by the NCBI GEO2R online tool. Based on the cut-off criteria of adjusted p ＜0.05 and |log2FC| ≥1, a total of 1422 DEGs, including 788 downregulated genes and 634 upregulated genes were detected. Figures 1A, B (volcano plot and heatmap) shows all the downregulated and upregulated DEGs.

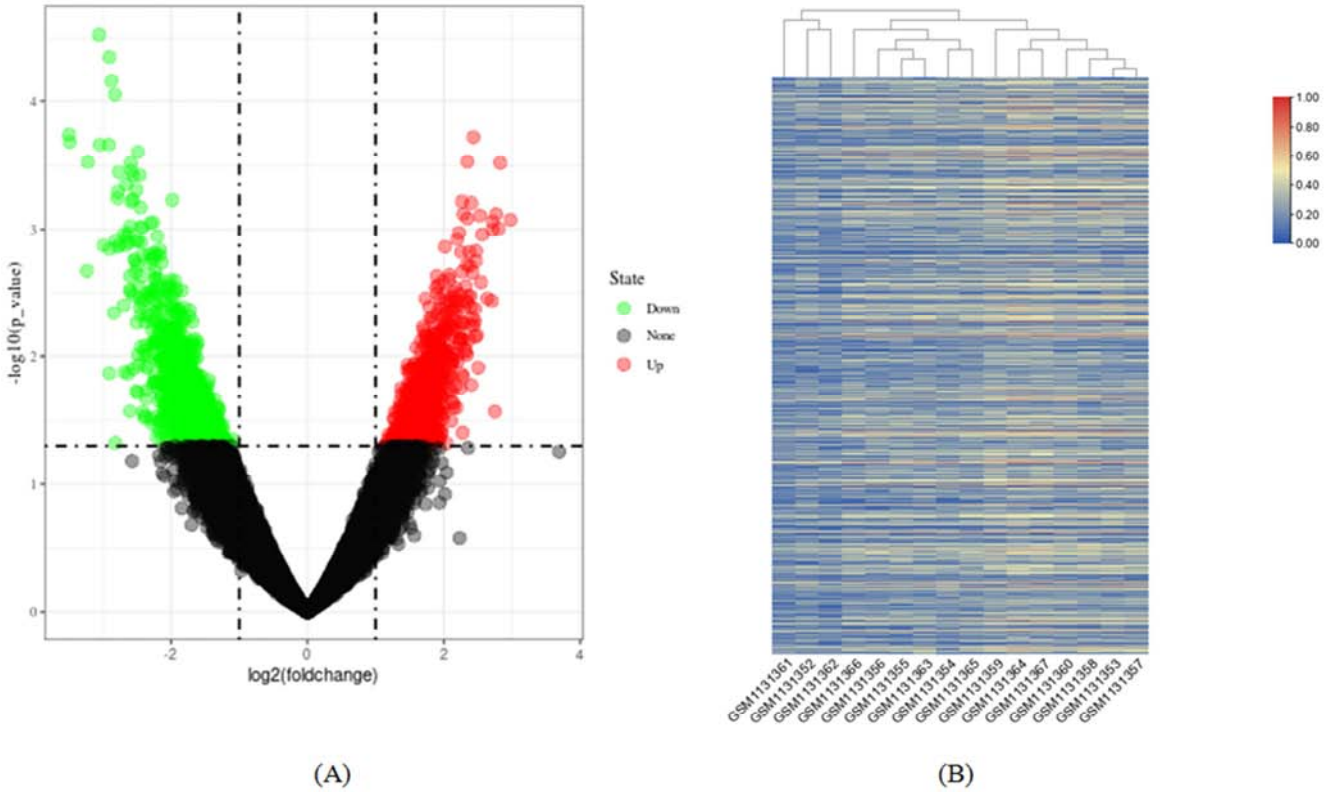

Figure 1. *Differentially expressed genes. (A) Volcano plot of all DEGs. Green dots represent down-regulated genes while the red dots represent upregulated genes, with p ＜0.05 and |log2FC| ≥1 as the cut-off. (B) Heat map of DEGs in the GSE46509 dataset.*

3.2. GO Function Enrichment Analysis of the DEGs

We used DAVID to analyze GO and KEGG pathways of the above DEGs. GO enrichment analysis results are shown in Tables A1-A3. The top 5 enriched terms in GO analysis are shown in Figures 2a-b. In biological processes (BP), the upregulated genes were mainly enriched in peptidyl-tyrosine phosphorylation (GO:0018108), response to lipopolysaccharides (GO:0032496), phosphatidylinositol-mediated signaling (GO:0048015), potassium ion transmembrane transport (GO:0071805), and phosphatidylinositol phosphorylation (GO:0046854). The downregulated genes were enriched in DNA-template negative regulation of transcription (GO:0045892), transcription from RNA polymerase II promoter (GO:0006366), cilium morphogenesis (GO:0060271), anatomical structure morphogenesis (GO:0009653), and RNA processing (GO:0006396). For cell component (CC) enrichment analysis, upregulated genes were significantly enriched in the cytoplasm (GO:0005737), extracellular matrix (GO:0031012), focal adhesion (GO:0005925), proteinaceous extracellular matrix (GO:0005578), and protein-DNA complex (GO:0032993). Downregulated genes were significantly enriched in the nucleus (GO:0005634), intracellular (GO:0005622), nucleolus (GO:0005730), actin cytoskeleton (GO:0015629), and nuclear chromosome/telomeric regions (GO:0000784). In the enrichment analysis of molecular function (MF), upregulated genes were enriched in DNA binding (GO:0003677), sequence-specific DNA binding (GO:0043565), chromatin binding (GO:0003682), transcriptional activator activity (GO:0001077), and protein tyrosine kinase activity (GO:0004713). The downregulated genes were mainly enriched in protein binding (GO:0005515), transcription factor activity (GO:0003700), zinc ion binding (GO:0008270), nucleic acid binding (GO:0003676), and mRNA binding (GO:0003729).

3.3. KEGG Pathway Enrichment Analysis of the DEGs

KEGG pathway results are shown in Table A4. The identified upregulated DEGs were enriched in cell adhesion molecules (hsa04514), viral myocarditis (hsa05416), and adherens junction (hsa04520). Downregulated DEGs were enriched in focal adhesion (hsa04510) (Figure 3).

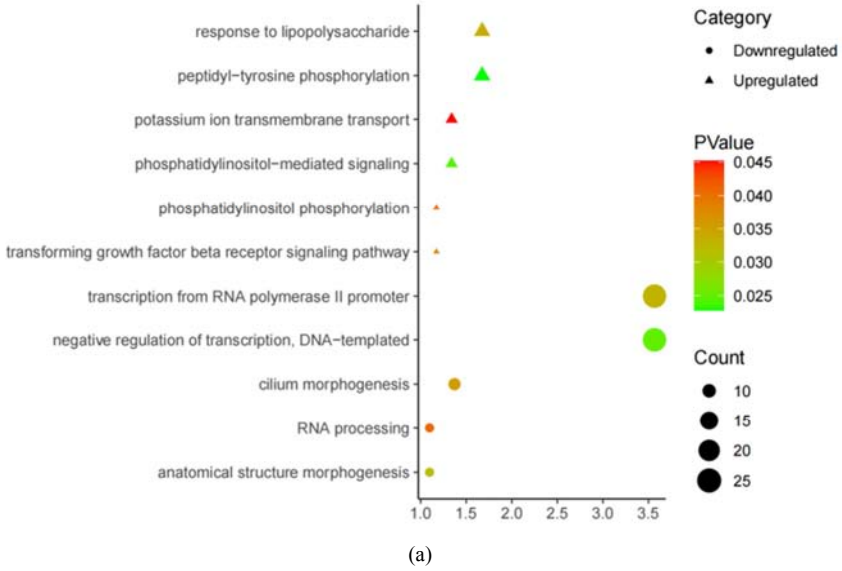

(a)

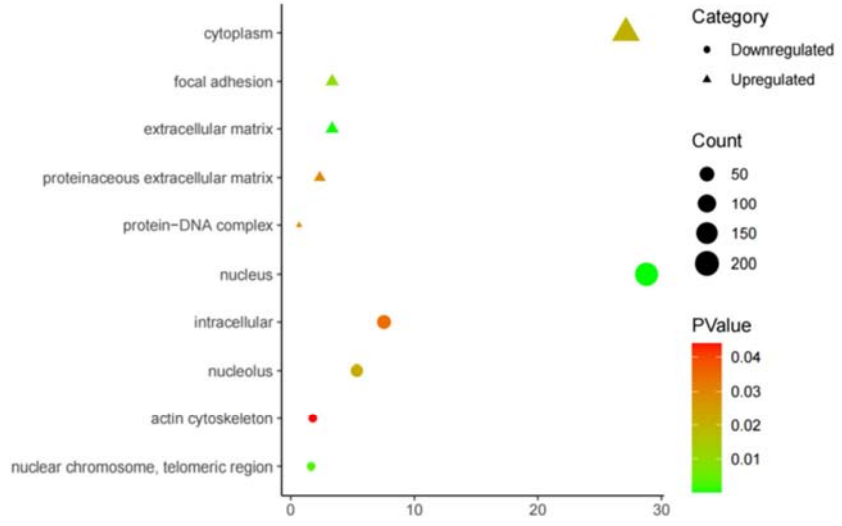

(b)

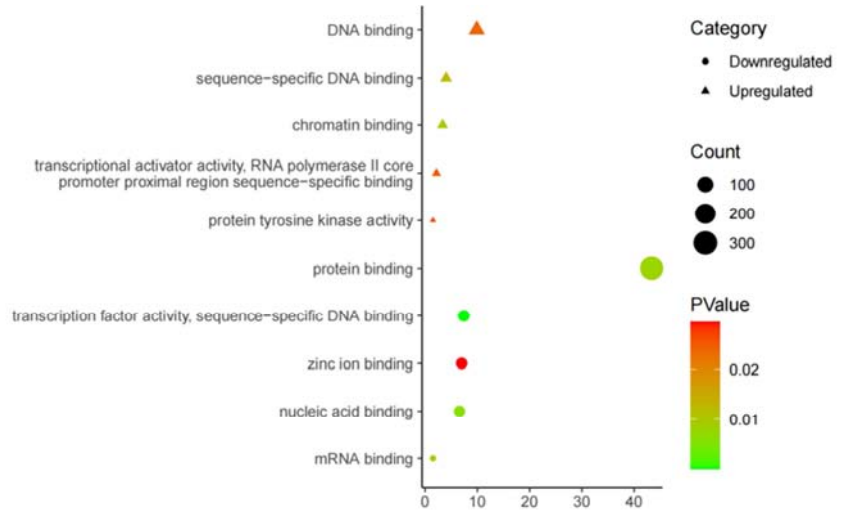

(c)

Figure 2. *GO function enrichment analysis of up-regulated and down-regulated differentially expressed genes. (a) Biological processes (BP). (b) Molecular functions (MF). (c) Cell component (CC).*

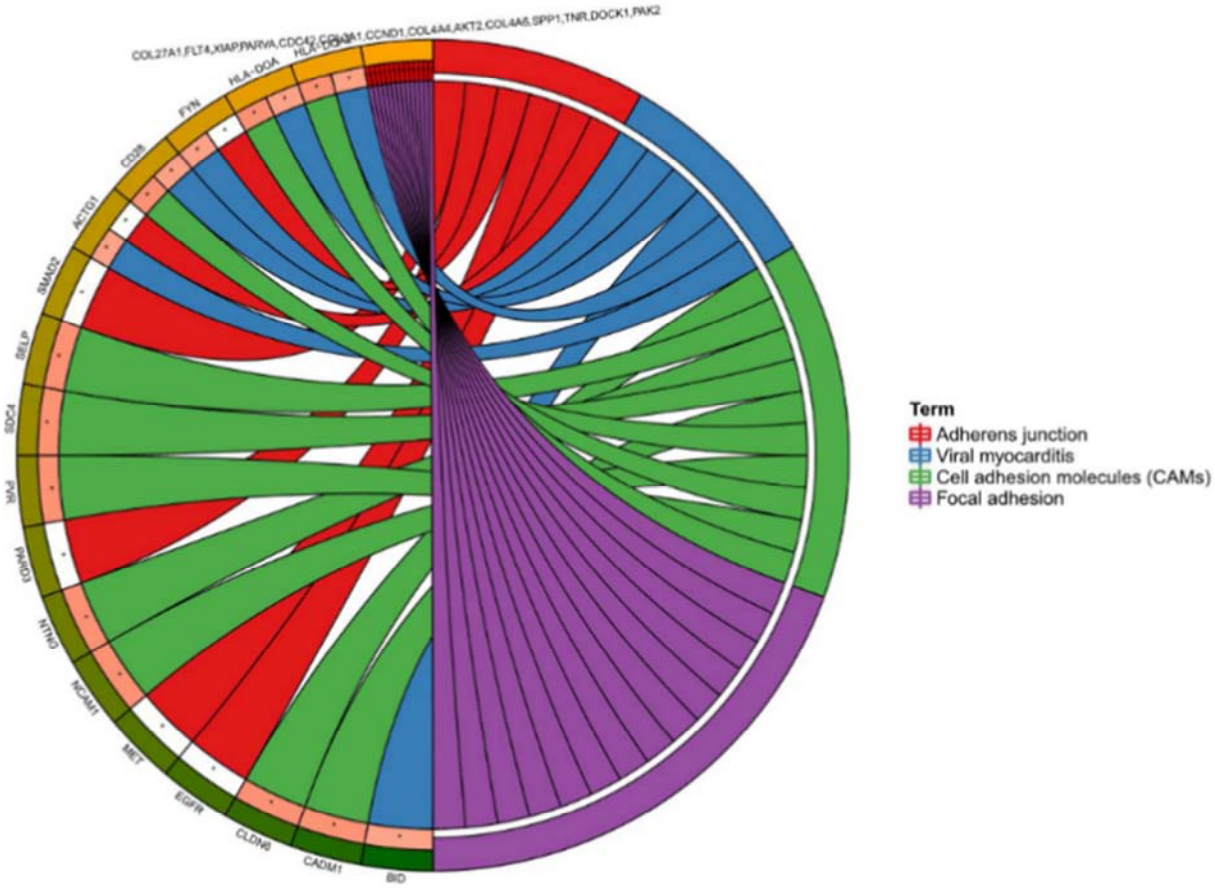

Figure 3. *KEGG pathway enrichment analysis of integrated DEGs.*

3.4. PPI Network Construction and Analysis of Modules

We imported the 1422 DEGs into the STRING database, the confidence score was set at the highest level (0.9) to obtain a PPI network. Based on STRING database information, MCODE was used to screen modules (degree cut-off = 2, node score cut-off = 0.2, k-Core = 5 and max. depth = 100). A total of 6 cluster modules were obtained from the PPI network. The top module with the highest score (score: 15) including 15 nodes (SOCS3, FBXO9, ASB17, FBXO10, ASB4, FBXL3, ASB12, UBE2V2, UBE2D3, AREL1, RNF144B, UBR1, UBE2O, UBE3D, UBE2G1) and 105 edges is shown in Figure 4. GO terms and KEGG pathway analyses of DEGs in the key module were performed using the ClueGO and CluePedia plugin (Figure 5 and Table A5). For the BP category, the most significantly enriched GO terms were regulation of mitotic recombination (GO:0006312), meiotic cell cycle process (GO:1903046), mitotic spindle organization (GO:0007052), organelle localization by membrane tethering (GO:0140056), and positive regulation of substrate adhesion-dependent cell spreading (GO:1900026). For the CC category, genes were enriched in the chromosomal region (GO:0098687), mRNA cleavage and polyadenylation specificity factor complex (GO:0005847), spliceosomal snRNP complex (GO:0097525), and clathrin-coated endocytic vesicle membrane (GO:0030669). In enrichment analysis of MF, genes were enriched in G protein-coupled peptide receptor activity (GO:0008528), exonuclease activity (GO:0004527), regulation of phosphatidylinositol 3-kinase activity (GO:0043551), and ubiquitin-like protein conjugating enzyme activity (GO:0061650). KEGG pathway analysis revealed that DEGs were significantly involved in mRNA surveillance pathway (KEGG:03015), neuroactive ligand-receptor interaction (KEGG:04080), Homologous recombination (KEGG:03440), Protein digestion and absorption (KEGG:04974), and Vasopressin-regulated water reabsorption (KEGG:04962).

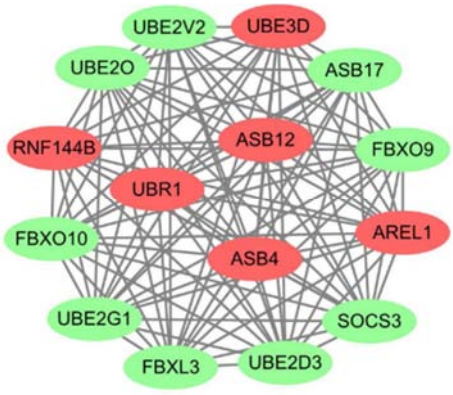

Figure 4. *The most significant module with the highest score in the PPI network. Red and green nodes indicate up-regulated and down-regulated genes, respectively.*

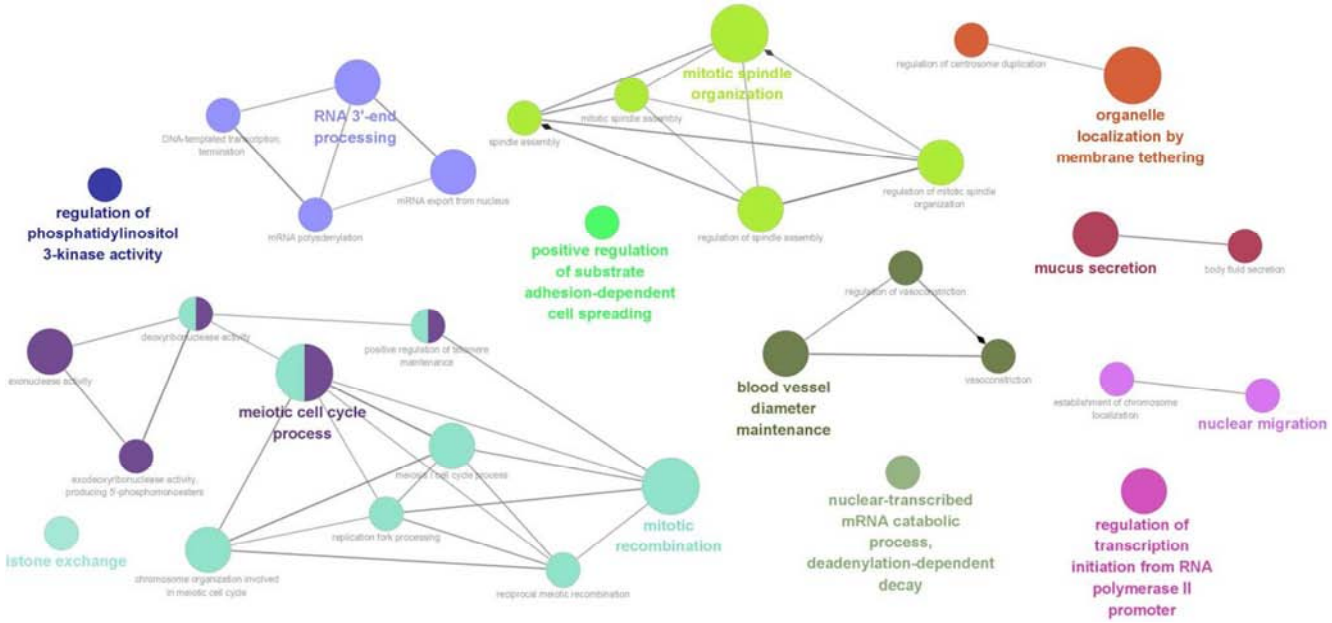
mitotic spindle organization
regulation of centrosome duplication
organelle localization by membrane tethering
RNA 3'-end processing
DNA-templated transcription, termination
mRNA export from nucleus
mRNA polyadenylation
mitotic spindle assembly
spindle assembly
regulation of mitotic spindle organization
regulation of spindle assembly
regulation of phosphatidylinositol 3-kinase activity
positive regulation of substrate adhesion-dependent cell spreading
mucus secretion
body fluid secretion
regulation of vasoconstriction
vasoconstriction
blood vessel diameter maintenance
establishment of chromosome localization
nuclear migration
deoxyribonuclease activity
exonuclease activity
positive regulation of telomere maintenance
meiotic cell cycle process
exodeoxyribonuclease activity, producing 5'-phosphomonoesters
histone exchange
replication fork processing
mitotic recombination
chromosome organization involved in meiotic cell cycle
reciprocal meiotic recombination
nuclear-transcribed mRNA catabolic process, deadenylation-dependent decay
regulation of transcription initiation from RNA polymerase II promoter

(a)

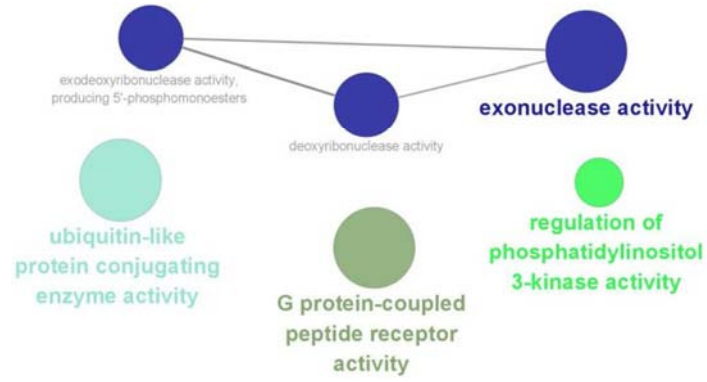
exodeoxyribonuclease activity, producing 5'-phosphomonoesters
deoxyribonuclease activity
exonuclease activity
ubiquitin-like protein conjugating enzyme activity
G protein-coupled peptide receptor activity
regulation of phosphatidylinositol 3-kinase activity

(b)

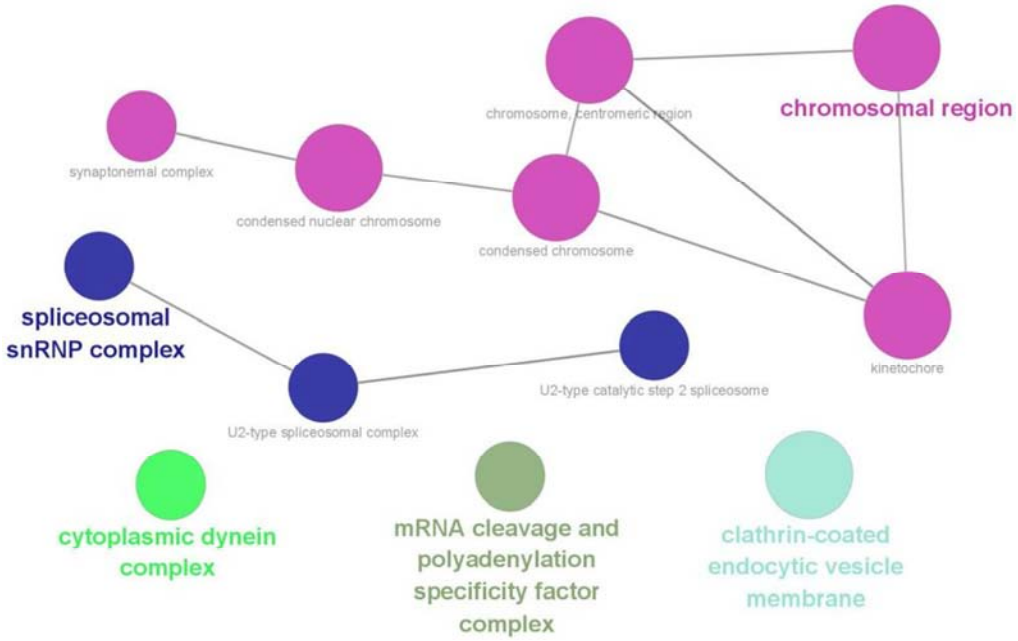
chromosome, centromeric region
chromosomal region
synaptonemal complex
condensed nuclear chromosome
condensed chromosome
spliceosomal snRNP complex
kinetochore
U2-type catalytic step 2 spliceosome
U2-type spliceosomal complex
cytoplasmic dynein complex
mRNA cleavage and polyadenylation specificity factor complex
clathrin-coated endocytic vesicle membrane

(c)

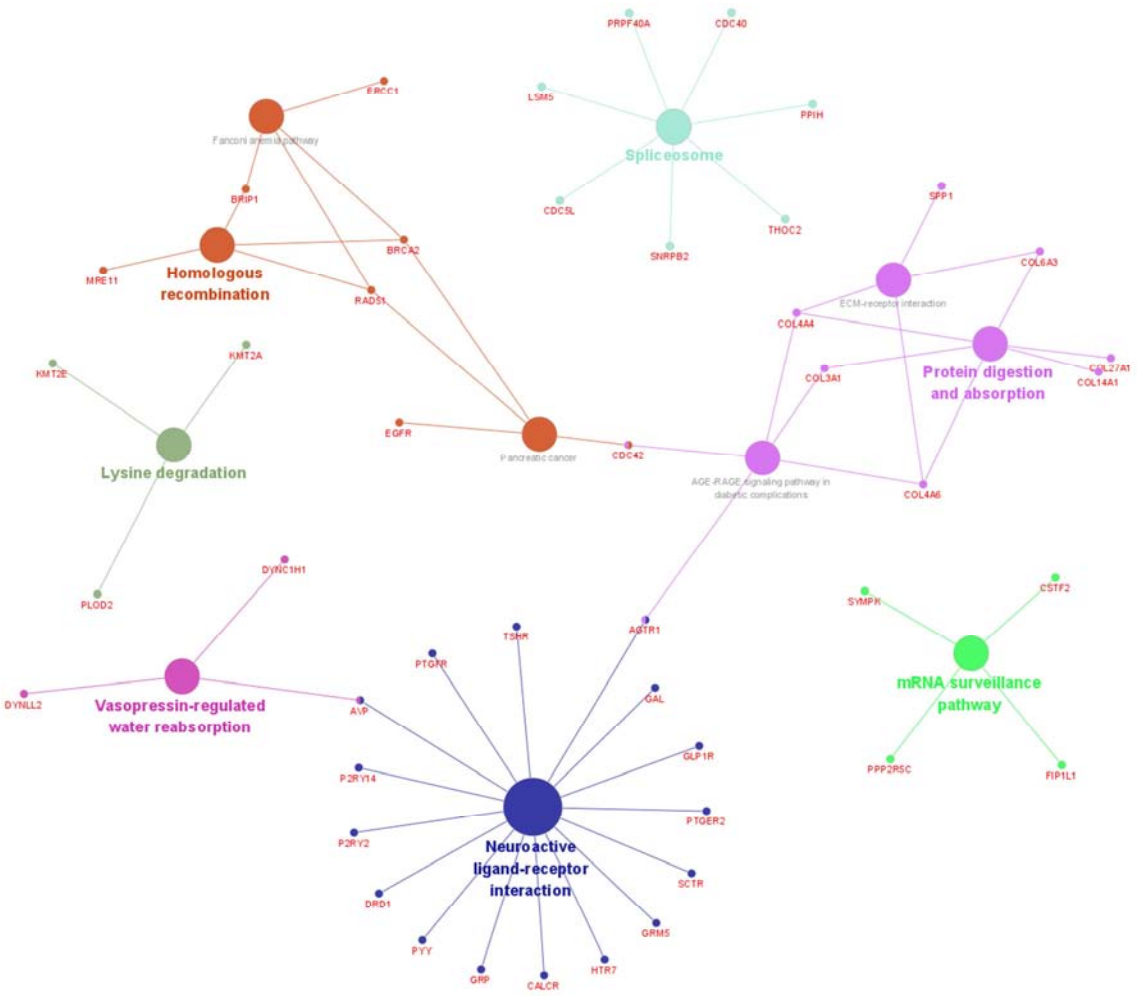

(d)

Figure 5. *GO analysis and KEGG pathway enrichment results for genes in all 6 modules. Node size indicates the term/pathway enrichment significance. Function related groups overlapped. (a) Biological process (BP). (b) Molecular function (MF). (c) Cell component (CC). (d) KEGG pathways.*

3.5. Biological Analysis of Hub Genes

To investigate important nodes in the biological networks, the Maximal Clique Centrality (MCC) analysis method of CytoHubba was used. The top 15 genes were identified as hub genes (Figure 6 and Table 1).

Table 1. *Top 15 hub genes. Sorted by Rank level.*

Rank	Name	Score
1	SOCS3	87178331534
2	FBXO9	87178331520
2	ASB17	87178331520
2	FBXO10	87178331520
2	ASB4	87178331520
2	FBXL3	87178331520
2	ASB12	87178331520
8	UBE2V2	87178291218
9	UBE2D3	87178291203
10	AREL1	87178291200
10	RNF144B	87178291200
10	UBR1	87178291200
10	UBE2O	87178291200
10	UBE3D	87178291200
10	UBE2G1	87178291200

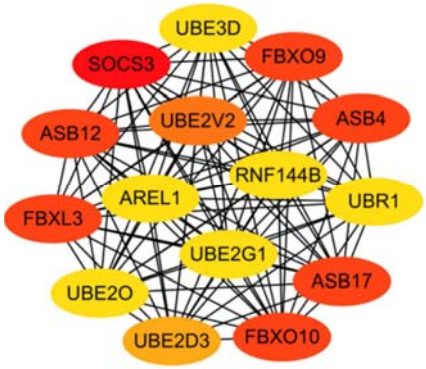

Figure 6. *Top 15 hub genes. Node color shows the Rank (the darker the color, the greater the Rank).*

Potential candidate target miRNAs of the top 5 genes from GSE46509 were predicted using TargetScan. Venn diagram analysis was performed for the predicted miRNAs (Figure 7). The intersection of the four genes was regarded as the ultimate target miRNAs. The four genes were; SOCS3, ASB4, FBXO9, and FBXO10. Using the Cytoscape software, we visualized the miRNA-mRNA network (Figure 8). We

hypothesized that miRNAs in the regulatory network play an important role in SZ pathogenesis. Therefore, hsa-miR-4514 was identified as a key miRNA. To elucidate on the functions of miRNAs, we analyzed miRNAs using the miRGen database. By matching miRNA precursor and transcription factor recognition sites, 12 target transcription factors regulating pre-miRNA expression were identified (E2F3, EGR1, NRF1, NR2C2, NFIL3, SP1, ETS1, KLF4, E2F4, THAP1, RFX2, and ZNF263), which correlated with hsa-miR-4514. Among these transcription factors, NRF1 was up-regulated while the remaining TFs were down-regulated in the GSE46509 dataset. Figure 9 shows the relationship between mRNA, miRNA, and TF. A TF-miRNA-mRNA regulatory network was constructed using Cytoscape. Figures 10a-b shows the miRNA-mRNA and TF-miRNA binding sites as predicted using TargetScan and miRGen.

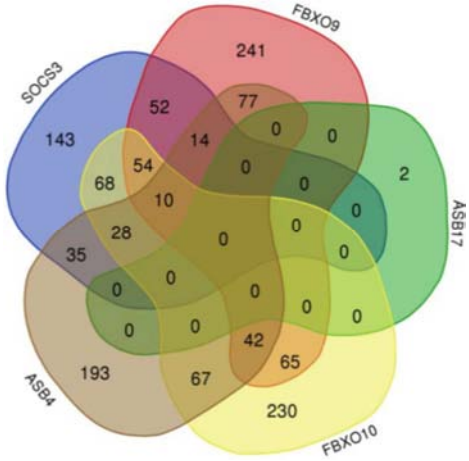

Figure 7. *Venn plot of five prediction results.*

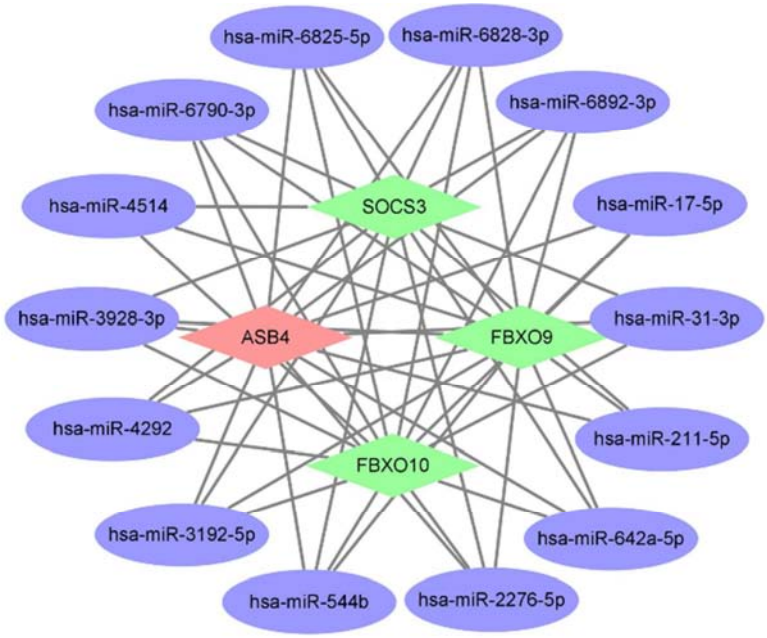

Figure 8. *Regulatory network of mRNAs-miRNA. Ellipses represent target miRNA while diamonds represent mRNA. Red and green indicate upregulated and downregulated mRNAs, respectively.*

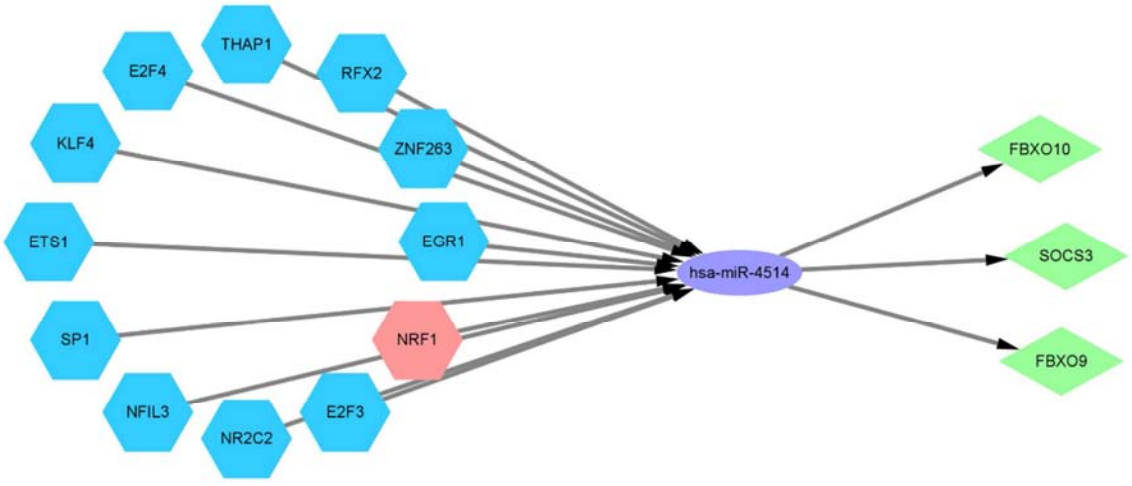

Figure 9. *Regulatory networks of key miRNA, mRNAs, and transcription factors. Hexagons represent TF, ellipses represent miRNA, while diamonds represent mRNA. Red and green colors indicate up-regulated and down-regulated genes in the GSE46509 dataset, respectively.*

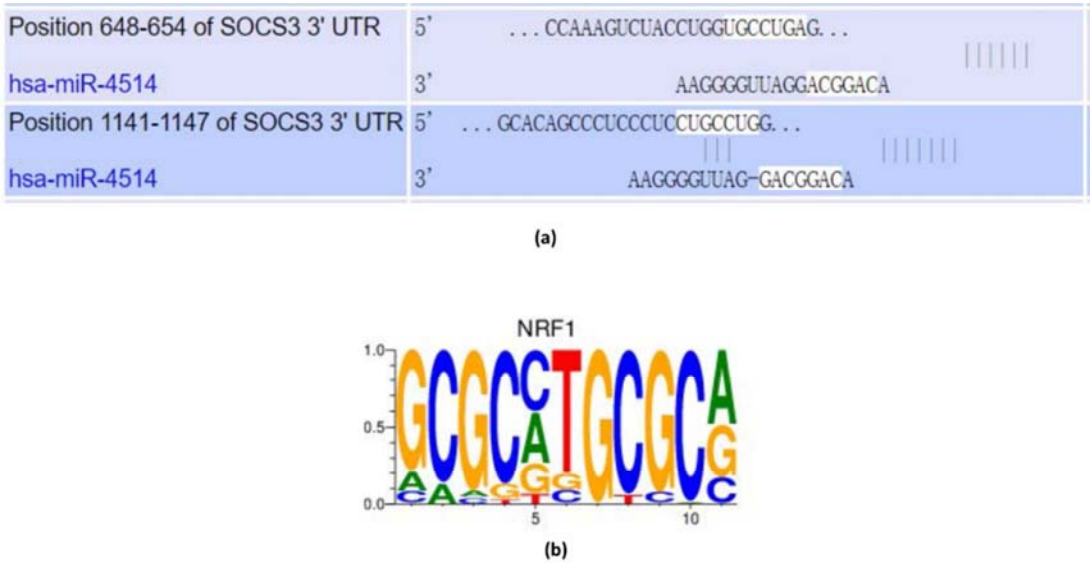

Figure 10. *Schematic presentation of the prediction of potential binding sites. (a) SOCS3 3'UTR-binding site for miR-4514. (b) Transcription factor, NRF1, binding sites on promoters of miR-4514.*

4. Discussion

Schizophrenia is a serious psychotic syndrome that is caused by a combination of genetic and environmental risk factors [22-24]. Various pathogenesis hypotheses for SZ, such as the dopamine hypothesis, the neurodevelopmental hypothesis, and the 5-HT hypothesis have been documented. However, the molecular mechanisms of SZ have not been fully elucidated. We used the bioinformatics approach to investigate differentially expressed genes that were associated with SZ development. A total of 1422 DEGs were identified in brain tissue samples of schizophrenia (Figure 1). To fully understand the role and mechanism of these DEGs, Gene ontology and KEGG pathway terms enrichment analyses utilizing the DAVID database and ClueGO plugin. respectively. We found a total of 36 GO_BP, 12 GO_CC, 6 GO_MF and 15 KEGG terms (Figure 2, Figure 3, and Figure 5). The DEGs were found to be associated with responses to RNA processing, mRNA binding, and cell adhesion molecules among others, which have previously been shown to be relevant to Schizophrenia progression [25-27].

RNA processing and mRNA binding are involved in SZ pathogenesis. Changes in common mRNA processing and translational modifications were found to be associated with schizophrenia [25]. Pri-miR-9-2 has a novel DGCR8-responsive RNA element (DRE) that promotes DGCR8-dependent pre-miRNA processing activity and is associated with an increased risk of schizophrenia [28]. DICER1 and AKT1 have functions in heterogeneous pathways, such as cell signaling and miRNA processing, and are dysregulated in SZ patients [29]. In addition, RBM3, SYNCRIP, ELAVL4, AGGF1, MRM1, BICD1, RBM6, and MRPL44 were enriched in RNA processing (Table A1). Among them, RBM3 is a proven potential marker for patients with affective disorders [30]. SYNCRIP [31], ELAVL4 [32], and BICD1 [33] are also associated with mental and neurological diseases. Another significantly enriched GO term was mRNA binding, which was enriched with FXR1, TPR, CELF4, SAMD4A, ELAVL4, LUC7L, DENR, THOC5, MRPS7, MRPL13, and EIF3A (Table A3). These findings imply that CELF4 and its homologs interact with RNA-binding proteins to regulate the expression of neurodevelopmental genes [26]. Functional polymorphisms of FXR1 have been reported as an important role in mental disorders, like schizophrenia [34]. These results are consistent with the findings of the present study.

To investigate hub genes of DEGs, a PPI network was conducted and those are the top 15 hub genes: SOCS3, FBXO9, ASB17, FBXO10, ASB4, FBXL3, ASB12, UBE2V2, UBE2D3, AREL1, RNF144B, UBR1, UBE2O, UBE3D, and UBE2G1 (Figure 6 and Table 1). SOCS3 (suppressors-of-cytokine-signaling 3), a key physiological regulator of the immune system, regulating T cells and antigen-presenting cells [35], was found to be enhanced by lncRNA, AC006129.1 in inflammation-mediated schizophrenia [36]. FBXL3 and ASB4 are closely associated with circadian rhythms [37, 38]. RNF144B [39], UBR1 [40], and UBE2G1 [41] play important roles in psychiatric disorders and neurodevelopmental diseases.

Importantly, miRNAs are associated with SZ pathogenesis by binding mRNAs, and inducing translational repression and/or mRNA degradation [34]. The miR-29 family, miR-34a-5p, and miR-132-3p in the humoral microcirculation are aberrantly expressed in central nervous system disorders such as schizophrenia [6]. Upregulated miR-7 and miR-181b are also associated with schizophrenia [7]. Thus, elucidation of the mRNA-miRNA network of the DEGs identified above may elaborate on the pathophysiology of schizophrenia [42]. Therefore, TargetScan was used to predict target miRNAs of the top 5 hub genes, and miR-4514 was shown to overlap the target miRNAs (Figures 7-8).

Studies on regulators of miRNA-mRNA network have revealed the role of transcription factors in influencing the

course of disease development through miRNA regulation, as evidenced in gastric cancer [43], rheumatoid arthritis [44], and cardiovascular diseases [45]. Investigation of gene regulatory systems driven by transcription factor-regulated miRNA precursor promoter regions may enhance our understanding of schizophrenia development [12]. We used miR-4514 to perform predictive analysis of transcription factors regulating the promoter region and found 12 TFs. Of those TFs, NRF1 (Neuregulin-1) was highly expressed in the selected datasets of this study. NRG1 is a putative schizophrenia susceptibility gene involved extensively in the central nervous system. NRG1 is localized at chromosome 8p12-21, and encodes one of the four proteins in the neuregulin family [46]. It may perform a variety of functions, including some aspects of neuronal migration, axon guidance, synaptic transmission, and neurite outgrowth [47, 48]. NRG1 was considered to be a putative SZ candidate gene in the central nervous system because of the expression of its target mRNAs and proteins was increased in the brain of SZ patients [49, 50]. Consistent with our findings from KEGG pathway analysis (Table A4), it has been suggested that a mechanism of NRG1 genetic association with schizophrenia may involve the molecular biology of cell adhesion [27]. Our results have shown that miR-4514 was upregulated by the highly expressed transcription factor (TF) NRF1, while several pivotal genes, such as SOCS3, FBBXO9, and FBBXO10, were downregulated (Figures 9-10). Therefore, a TF-miRNA-mRNA targeted regulatory network may have an crucial role in schizophrenia.

However, there are some limitations in this study. First, our source data were from brain samples of postmortem SZ patients. It is difficult to obtain brain samples in clinical settings. Then, these results are only based on bioinformatic analysis. Thus, a series of vivo and animal experiments need to be performed to validate the results of this study in the future.

5. Conclusion

In conclusion, 1422 DEGs, 15 hub genes, and 1 TF-miRNA-mRNA regulatory network were identified. SOCS3, FBBXO9, FBBXO10, NRF1, as well as miR-4514 may have potential application value in the clinical practice of schizophrenia. And this present study may have a reference value for further researches.

Authorship Confirmation Statement

The authors claim that none of the material in the paper has been published or is under consideration for publication elsewhere.

Author Contributions

YL conceived this study. YZ and ZW coordinated and directed the project. YL and LY acquired and analyzed the data. YL, SJ wrote the paper. XM, QL, YT, ZC were of immense help in the preparation of the manuscript. All authors read and approved the final manuscript.

Author Disclosure Statement

The authors declare that they have no conflicts of interest.

Funding

This study was supported by National Natural Science Foundation of China (No. 81960254 and 81760253), Yunnan health training project of high level talents (No. L-2017021 and H-2017064), and Joint special fund of Applied Fundamental Research of Kunming Medical University granted by Science and Technology Office of Yunnan, grant no. 2018FE001-(009).

Appendix

Table A1. *Significantly enriched GO terms of DEGs (Biological process).*

GO ID	Term	P-value	Genes
upregulated genes			
GO:0050860	negative regulation of T cell receptor signaling pathway	0.000933	DUSP3, PAWR, PTPN22, BTNL2, EZR
GO:0042554	superoxide anion generation	0.005653	NCF2, NOX3, SOD2, NOX1
GO:1901379	regulation of potassium ion transmembrane transport	0.006926	KCNE1, KCNIP2, KCNIP3, KCNAB1
GO:0061337	cardiac conduction	0.006964	CACNG8, KCNE1, CACNB4, KCNIP2, KCNJ12, KCNIP3
GO:0060449	bud elongation involved in lung branching	0.013880	YAP1, FGFR2, FGF10
GO:0048536	spleen development	0.015453	ADAM17, CDKN2B, PPP2R3C, PRKDC, FGF10
GO:0006491	N-glycan processing	0.015712	EDEM3, MAN1A2, ST8SIA4, USF3
GO:0031659	positive regulation of cyclin-dependent protein serine/threonine kinase activity involved in G1/S transition of mitotic cell cycle	0.018179	ADAM17, EGFR, FGF10
GO:0051592	response to calcium ion	0.019689	TPH2, PCDH15, ANXA11, ITPR3, EGFR, TTN
GO:0018108	peptidyl-tyrosine phosphorylation	0.022792	EPHA4, ZAP70, EFEMP1, CSF2, FYN, MET, EGFR, FGFR2, TTN, FGF10
GO:0048754	branching morphogenesis of an epithelial tube	0.023005	MMP14, MET, GLI2, FGF10
GO:0070536	protein K63-linked deubiquitination	0.023005	OTUB2, CYLD, ATXN3, OTUD7B
GO:0048015	phosphatidylinositol-mediated signaling	0.024400	KITLG, CD28, FYN, PIK3C2A, EZR, EGFR, FGFR2, FGF10

GO ID	Term	P-value	Genes
GO:0007126	meiotic nuclear division	0.025778	RAD51, TUBGCP3, HORMAD2, SMC1A
GO:0045740	positive regulation of DNA replication	0.025907	KITLG, CSF2, EGFR, GLI2, FGF10
GO:0032496	response to lipopolysaccharide	0.033592	SELP, ADAM17, MAPKAPK3, PTGER2, LTA, TNFRSF10B, CCR7, PTPN22, SOD2, FGF10
GO:0045060	negative thymic T cell selection	0.033859	ZAP70, CD28, CCR7
GO:0016575	histone deacetylation	0.034760	RBBP4, SAP30L, BRMS1L, MORF4L2, BAZ2A
GO:1903507	negative regulation of nucleic acid-templated transcription	0.037215	YAP1, NEUROD2, CASP8AP2, KCNIP3, HOXC6
GO:0007179	transforming growth factor beta receptor signaling pathway	0.037790	SMAD2, COL3A1, ITGB5, PARD3, FOXH1, LTBP2, TAB1
GO:0045931	positive regulation of mitotic cell cycle	0.038574	FOXA1, DUSP3, USP2, FGF10
GO:0046854	phosphatidylinositol phosphorylation	0.041297	KITLG, CD28, FYN, PIK3C2A, EGFR, FGFR2, FGF10
GO:0015992	proton transport	0.042417	SLC35A3, MFSD3, SLC4A11, ATP5O, NOX1
GO:0071805	potassium ion transmembrane transport	0.045174	KCNE1, KCNG4, KCNK9, KCNIP2, KCNIP3, KCNAB1, NALCN, SLC12A9
GO:0055072	iron ion homeostasis	0.045974	STEAP3, HFE, SFXN4, SOD2
GO:0007409	axonogenesis	0.048910	NTNG1, GSK3B, SLITRK2, PARD3, LRRN1, FMOD, FGFR2
GO:0008016	regulation of heart contraction	0.049918	GLP1R, KCNIP2, KCNJ12, CELF2
GO:0048701	embryonic cranial skeleton morphogenesis	0.049918	SMAD2, MMP14, ALX3, FGFR2
downregulated genes			
GO:2000146	negative regulation of cell motility	0.002559	SPOCK3, FBLN1, AP1AR, GATA3
GO:0010975	regulation of neuron projection development	0.003021	CCDC88A, SFRP1, AVIL, GATA3, KLK6
GO:0045725	positive regulation of glycogen biosynthetic process	0.011968	DYRK2, AKT2, INSR, SORBS1
GO:0021853	cerebral cortex GABAergic interneuron migration	0.014819	LHX6, DRD1, FEZF2
GO:2000271	positive regulation of fibroblast apoptotic process	0.014819	SFRP1, STK17B, TP63
GO:0030856	regulation of epithelial cell differentiation	0.020298	STAT5B, FOXJ1, ASCL1
GO:0007585	respiratory gaseous exchange	0.024549	NDST1, UCP3, PBX3, COX11, HNMT
GO:0045892	negative regulation of transcription, DNA-templated	0.024794	L3MBTL1, ZNF253, YWHAB, GATA3, ASCL1, HDAC9, WNT11, SIN3A, SMYD1, ZNF227, FEZF2, SOX7, HES2, TP63, ZNF540, UBE2I, CBX5, CBX3, FOXN3, PA2G4, SFRP1, ZNF93, KAT6B, TRAF6, MYF6, LIMS1
GO:0006729	tetrahydrobiopterin biosynthetic process	0.026481	QDPR, GCH1, PCBD2
GO:0006631	fatty acid metabolic process	0.027553	STAT5B, AASDH, UCP3, THEM5, ABHD5, HADH
GO:0016485	protein processing	0.030866	CPD, XPNPEP3, PIK3C3, PPP2R5C, PCSK6, ASPRV1, KLK6
GO:0009653	anatomical structure morphogenesis	0.031801	EFNB2, KRT35, TRIM13, GATA3, TBX6, BICD1, LYVE1, HOXA4
GO:0006366	transcription from RNA polymerase II promoter	0.032840	DLX2, KMT2A, HSF2BP, GATA3, GATA1, POLR2A, TCEB3, PKNOX1, NKX6-1, FEZF2, TP63, EGR1, STAT5B, LMO4, FOXJ2, PBX3, PAX3, FOXJ1, ETV1, MED4, ETV6, NFKB2, MYF6, TFAM, TAF5, LCORL
GO:0010165	response to X-ray	0.034197	CCND1, ERCC1, BRCA2, TP63
GO:0060271	cilium morphogenesis	0.035647	SPAG16, RAB1A, AVIL, TMEM67, IQUB, FOXJ1, PARVA, CFAP54, SSX2IP, SEPT2
GO:0021987	cerebral cortex development	0.036443	COL3A1, FAT4, ASCL1, GART, MCPH1, PPP1R9B
GO:0006396	RNA processing	0.040648	RBM3, SYNCRIP, ELAVL4, AGGF1, MRM1, BICD1, RBM6, MRPL44
GO:0034063	stress granule assembly	0.040753	DYNC1H1, OGFOD1, BICD1
GO:0008286	insulin receptor signaling pathway	0.043164	AKT2, INSR, IRS4, SORBS1, PIK3C2A, GPLD1, RPE65
GO:0000188	inactivation of MAPK activity	0.047531	DUSP4, DUSP21, GPS1, DUSP6

Table A2. *Significantly enriched GO terms of DEGs (Molecular function).*

GO ID	Term	P-value	Genes
upregulated genes			
GO:0005201	extracellular matrix structural constituent	0.008887	FBN2, COL3A1, COL27A1, COL14A1, LAMA4, ANOS1, FBLN1
GO:0003682	chromatin binding	0.009163	YAP1, SMAD2, TEX10, ATRX, PBX2, GATA2, SMC1A, EGFR, TDRD3, GLI2, FABP1, MEIS1, RAD51, TADA2A, RFX4, POLD1, SVEP1, PATZ1, ZMYND11, GABPA
GO:0043565	sequence-specific DNA binding	0.012351	FOXA1, ZNF396, KCNIP3, FOXH1, PBX2, HSFY2, CDC5L, TAF1L, OTP, NR1D2, NR2F2, CTCFL, GLI2, SNAPC1, HNF4A, ALX3, ZSCAN12, SOX6, HOXB8, MIXL1, GABPA, LHX9, FOXA2, HOXC6
GO:0005138	interleukin-6 receptor binding	0.013682	ADAM17, ERAP1, IL6ST
GO:0004571	mannosyl-oligosaccharide 1,2-alpha-mannosidase activity	0.017923	EDEM3, MAN1A2, USF3

GO ID	Term	P-value	Genes
GO:0003677	DNA binding	0.023962	PRDM8, KDM5A, FOXA1, PHF20, ZBTB20, OTUD7B, HNF4A, ZNF527, ZNF326, ZNF644, SOX6, ZNF443, GABPA, FAAP100, TIGD2, CERS4, KLF12, H2AFY, APLP2, ZNF160, ATRX, FOXH1, PROX2, RUNX3, ZFX, WDR76, TOPORS, ZNF91, RFX4, ZNF780B, ZNF780A, BAZ2A, HMBOX1, POLD1, SAP30L, G3BP1, PATZ1, HOXC6, SMAD2, CASP8AP2, NFYA, KCNIP3, CDC5L, NR2F2, USF3, SOD2, CTCFL, POU6F1, KLF7, MLLT10, MEIS1, RAD51, ZBTB6, TADA2A, ZNF37A, ZNF416, MEIS3P1, LHX9, FOXA2
GO:0046934	phosphatidylinositol-4,5-bisphosphate 3-kinase activity	0.024794	KITLG, CD28, FYN, EGFR, FGFR2, FGF10
GO:0001077	transcriptional activator activity, RNA polymerase II core promoter proximal region sequence-specific binding	0.025191	FOXA1, SMAD2, NRF1, GATA2, CTCFL, GLI2, MEIS1, HNF4A, RFX4, PATZ1, MEF2D, MIXL1, GABPA
GO:0004713	protein tyrosine kinase activity	0.026443	EPHA4, ZAP70, CSF2, FYN, MET, EGFR, FGFR2, TTN, FGF10
GO:0016175	superoxide-generating NADPH oxidase activity	0.033394	NCF2, NOX3, NOX1
GO:0019838	growth factor binding	0.034463	FGFBP2, LTBP2, LIFR, IL6ST
GO:0015075	ion transmembrane transporter activity	0.039377	GJA1, SFXN4, ATP11B
GO:0005184	neuropeptide hormone activity	0.045130	POMC, PYY, GAL, GRP
GO:0008047	enzyme activator activity	0.046930	DBF4, MMP17, CFLAR, TAB1, SAE1
downregulated genes			
GO:0003700	transcription factor activity, sequence-specific DNA binding	0.000128	MYT1L, SIN3A, ZNF567, PKNOX1, SOX7, LZTS1, TP63, HOXA4, ZNF200, TEAD4, ZNF480, LMO4, PAX3, ETV1, ZNF75D, ZNF16, ETV6, ZNF717, ZNF93, TFAM, IRF5, ZNF677, ZNF780A, ATF6, ZNF793, L3MBTL1, DLX2, KMT2A, GATA3, ZNF3, ASCL1, GATA1, ZNF821, ZNF227, SCAND1, NKX6-1, ZIM2, ZNF585A, ZNF540, EGR1, STAT5B, STAT1, PBX3, FOXJ1, PA2G4, FOXN3, TBX6, NFKB2, ZNF33A, CNOT7, ZNF37A, MYF6, LHX6, TAF5
GO:0003676	nucleic acid binding	0.005771	ZNF793, N6AMT1, ZNF473, ZNF253, RBM47, TMEM161B, GPATCH2, CELF4, GPATCH4, ZNF3, TSEN2, ZCCHC14, RBM3, SYNCRIP, BRIP1, ZNF507, ZNF407, ZNF208, ZNF701, ZNF426, ZNF821, ZNF227, ZNF567, ENPP3, ZNF664, ZIM2, ZNF740, ZNF200, ZNF585A, ZNF684, ZNF540, DDX18, NIFK, ZNF480, MTERF2, RNASE4, ZNF75D, ZNF33A, GPANK1, ZNF70, CNOT7, ZNF717, ZNF93, AGGF1, ZNF677, ZNF780A, ZNF233, CPEB4
GO:0003729	mRNA binding	0.007856	FXR1, TPR, CELF4, SAMD4A, ELAVL4, LUC7L, DENR, THOC5, MRPS7, MRPL13, EIF3A
GO:0005515	protein binding	0.007961	TRAF3IP2, DCAF8, GPATCH4, HSF2BP, RCBTB2, GLS, ALKBH3, NDST1, UBASH3B, ZMIZ2, AKT2, CHORDC1, PDK3, LUC7L, DENR, EPHB2, CEP97, SOX7, TP63, FBXO9, DDX18, KRT4, SCAF11, COG2, MED4, TMEM170A, CDC40, MED6, ZNF16, TWSG1, SFRP1, BCAM, BIN2, DAAM1, AGTR1, TRIM13, TFAM, CD226, SIK2, ATF6, L3MBTL1, TMEM185A, TEX264, CDCA4, SDC2, GATA3, GATA1, GSPT2, MRPL13, KLK6, FXR1, NHLH2, PCNX4, BRIP1, FIGNL1, HIST1H3H, ZNF821, TRPM8, HBQ1, CEP76, ELANE, SNX5, PLK4, STAT5B, EGR1, NDFIP2, FAM9A, FZD2, HIST1H4L, INSR, CYP4F2, PARVA, PA2G4, GKAP1, RPL27A, CALU, FBXL3, STRN, FAT4, GRAP, CTRC, CDK14, SLC22A7, CPEB4, SETD2, CLIC3, MSTN, FAF1, OTUD7B, BRCA2, LARP1B, TRIM8, SYNCRIP, CRTAC1, DLGAP3, TEAD4, LRRC45, PBRM1, NCOA3, STRBP, PAX3, PRPF40A, TMEM173, TERF2, DYNLL2, MRPL44, CTU2, RAD51D, TLR6, VAMP4, ERGIC2, VAMP3, ZNF473, CRB1, ZNF593, GPS1, ADAM22, XIAP, NOL9, AKAP5, ZNF3, ASCL1, TANK, TMEM67, UCP3, SPP1, TCEB3, MFN1, RHO, TLDC1, ZNF227, SCAND1, CCL18, PAK2, SVIL, DYNC1H1, SLF1, GCH1, STAT1, CCL20, DNAJC5B, GLYCTK, SUSD2, SAMD4A, SORBS1, LYVE1, LILRB4, SVIP, FABP2, COL3A1, LYRM2, NMNAT1, AGGF1, RAD1, FAM46D, LIMS1, CARS, N6AMT1, RAB3C, UBE2D3, IRS4, TSEN2, CCND1, FNTA, OSBP, ZNF567, LZTS1, POSTN, SPINK7, LMO4, HBE1, FBXO10, THOC5, SRCIN1, GPANK1, PACRGL, PHOSPHO2, TBC1D20, SLC9A7, ILVBL, KAT6B, TIPRL, UBE2V2, NHP2, PPIH, ZNF555, IL6ST, S100A8, DGKI, HIST1H2BC, KLHL18, REG3A, DLX2, FAM114A1, KMT2A, SLC41A2, BTF3L4, NREP, PDS5A, LPP, KIR2DL4, EFNB2, KIAA1524, SOCS3, SYCE1, BAG5, KIF3B, CLEC7A, TPR, NPHP1, THEM5, ABL2, SMYD1, STAP1, ZNF426, DRD1, BCL2L14, MDN1, ZNF540, UBE2I, CBX5, KIRREL, CBX3, MUC17, FOXN3, LSM5, NFKB2, PTPRD, GH1, KIF18A, LRCH1, CNOT7, DLG5, LHX6, UBE2O, LHX8, PICALM, DOCK5, GPSM2, HSPB9, DYRK2, YWHAB, HSPB8, FLT4, HP1BP3, FAM208B, BICD1, PPP1R9B, RBM3, SIN3A, IQUB, POLI, RBM6, SUN1, TTC32, DIS3, ACTR6, MMP2, ETV1, PPP2R5C, POMGNT1, SEPT2, ETV6, WRAP73, DUSP21, MEP1A, TRAF6, MMRN2, IRF5, NDUFS1, PIK3C3, LCORL, DOCK1, SSX2IP, MCPH1, OTUB2, RAB1A, NUTM1, USP15, CATSPER2, GOSR2, RAP1GDS1, ZBTB43, GTPBP10, HDAC9, MRM1, AURKB, CDC42, WNT11, POLR2A, GNG4, PCED1A, RGS20, PCBD2, TRIM49, LRRC8B, PDLIM7, CMTM3, NIFK, ERAP1, FOXJ2, LCA5, FOXJ1, TBX6, ATP2B1, GFER, TPCN2, TNRC6C, WEE1, ERCC1, TAF5, TRIM38, NAA15, P4HB, PTPN4, EIF3A

GO ID	Term	P-value	Genes
GO:0008270	zinc ion binding	0.029352	ZNF253, KDM5D, MYT1L, OTUD7B, ZCCHC14, ADAMTSL1, TRIM8, NPEPPS, ZMIZ2, ZNF407, ZNF208, CHORDC1, RAG2, ADAMTS8, APOBEC2, SCAF11, LMO4, SLC30A5, MMP2, ZNF75D, ZNF93, MEP1A, KAT6B, TRAF6, TRIM13, S100A8, L3MBTL1, ZNF593, KMT2A, XIAP, GATA3, ZNF3, LPP, GATA1, ABLIM2, PGGT1B, TRIM49, PDLIM7, ZIM2, EGR1, GCH1, ERAP1, RNF145, RNF148, CPD, TLL2, LHX6, RTN4IP1, TRIM38, LIMS1, LHX8
GO:0034452	dynactin binding	0.032882	SPTBN5, BICD1, SNX5
GO:0000900	translation repressor activity, nucleic acid binding	0.040228	ZNF540, CELF4, CPEB4
GO:0000976	transcription regulatory region sequence-specific DNA binding	0.040432	EGR1, SIN3A, FOXJ1, GATA3, ATF6, GATA1
GO:0030742	GTP-dependent protein binding	0.042088	CDC42, RAB3C, GCH1, RAPGEF5

Table A3. *Significantly enriched GO terms of DEGs (Cell component).*

GO ID	Term	P-value	Genes
upregulated genes			
GO:0031012	extracellular matrix	0.000428	FBN2, SPON1, COL14A1, PRKDC, LAMA4, LTBP4, FBLN1, LTBP2, ATP5O, ACTG1, COL3A1, MMP14, EFEMP1, MMRN2, MMP17, COL6A3, VIM, FMOD, FGFR2, FGF10
GO:0005925	focal adhesion	0.009629	GIT2, ITGB5, SDC4, MME, SNAP23, ARHGAP26, PVR, EGFR, ACTG1, APBB1IP, MMP14, GJA1, ADAM17, RFWD2, G3BP1, TRIP6, CAT, VIM, EZR, SNTB1
GO:0005737	cytoplasm	0.020390	GLTP, VEZT, PANK2, STEAP3, NCF2, UBE3D, CTNND2, DCAF8, AQP4, PVR, FAM110A, RASSF3, PTTG2, HABP4, SVEP1, GNAT1, FAAP100, EPHA4, SDS, AKR1E2, ANXA11, RUNX3, DCTD, RUFY1, STX1B, ADAM17, SPATA17, MAPKAPK3, ARMC3, SHPK, NAAA, MT1G, PLAA, TSSK3, EZR, GPLD1, DSC3, KMT2E, ZNF396, CDCA7, PCDH15, ITPR3, BAZ2A, UBR1, ABHD5, CD79B, KIAA1524, ATXN3, HMBOX1, FXR2, FGGY, MYO6, G3BP1, CEP70, SYMPK, RIMKLA, IP6K3, NXNL2, CNTLN, HOXC6, GSTM4, SMAD2, BTBD17, DNAH14, KLHDC1, STYX, RASSF7, TDRD3, SELP, MOB1B, TSGA10, MLLT10, NDUFAF6, TRIP6, NOX3, SPATS2L, PCDHB4, TUBGCP3, TAB1, MAP3K13, FGFR2, KDM5A, GSK3B, PIWIL4, PHF20, CELF2, SNAP23, OTUD7B, PTPN22, ARHGAP5, PIK3C2A, AKAP13, GRM5, CA1, ACP6, AKAP14, HNF4A, KYNU, RBPMS2, KLF12, DUSP3, MME, DESI2, TEX10, PAWR, IL16, KCNAB1, PPHLN1, SMC1A, KIF27, RNF144B, ZAP70, MMP14, FBP1, YAP1, PLEKHH2, SAMD9, PRUNE2, HSFY2, FIGN, AFP, EGFR, ALS2CL, EXOSC4, PPP2R3C, POLD1, FAM120A, ANKAR, CCL3, NCAM1, CHML, PDLIM5, BID, FNIP1, MEF2D, MAPK4, CASP8AP2, ATE1, CDKN2B, KCNIP2, GINS4, CDC5L, CFLAR, CDC42BPA, CPPED1, CTCFL, POMC, FABP1, KITLG, RAD51, EIF3K, RFWD2, CR1L, CAMK4, RFWD3, OTULIN, FAM98B, ASB4, VIM, SNTB1, FOXA2, UMODL1
GO:0032993	protein-DNA complex	0.028500	KDM5A, NFYA, KCNIP3, CDC5L
GO:0005578	proteinaceous extracellular matrix	0.029297	FBN2, SPON1, COL14A1, CRISP3, LTBP4, FBLN1, LTBP2, EFEMP1, ADAMTSL3, MMP17, ANOS1, COL6A3, FMOD, GPLD1
GO:0043020	NADPH oxidase complex	0.039694	NCF2, NOX3, NOX1
GO:0042581	specific granule	0.046095	CRISP3, SNAP23, ANXA11
downregulated genes			
GO:0005634	nucleus	0.000298	CCNJ, MYT1L, DCAF8, DCAF6, ALKBH3, ALKBH2, UBASH3B, ZMIZ2, AKT2, OGFOD1, PKNOX1, SOX7, TP63, HOXA4, KRT4, SCAF11, MED4, MED6, ZNF16, ZNF717, TFAM, SIK2, ATF6, L3MBTL1, CDCA4, CDCA7, GATA3, GATA1, NHLH2, EPB41L5, BRIP1, FIGNL1, ZNF701, HIST1H3H, ZNF821, STAT5B, EGR1, FAM9A, HIST1H4L, DDIAS, PBX3, PARVA, PA2G4, PARP15, ZNF37A, FBXL3, CDK14, CPEB4, SPAG16, ZNF253, SETD2, CLIC3, FAF1, ADK, OTUD7B, BRCA2, LARP1B, SYNCRIP, FEZF2, DUSP4, TEAD4, NCOA3, STRBP, TERF2, DYNLL2, MRPL44, RAD51D, ZNF780A, CYLC2, RAPGEF5, ERGIC2, ZNF233, ZNF593, XIAP, ZNF3, ASCL1, TCEB3, ZNF227, SCAND1, ZIM2, ZNF585A, SVIL, TRMT10A, SLF1, GCH1, STAT1, SORBS1, ZNF33A, ZNF70, NMNAT1, STK17B, RAD1, MPO, NPEPPS, CCND1, ZNF208, OSBP, TNR, ZNF567, RAG2, FADS1, ZNF200, ZNF684, RALGAPA1, SLC30A5, THOC5, ZNF93, KAT6B, UBE2V2, ZNF677, ZNF555, HIST1H2BA, S100A8, DGKI, HIST1H2BC, ZNF793, DLX2, KMT2A, NREP, ABHD5, PDS5A, LPP, BAG5, TPR, SMYD1, STAP1, ZNF426, DRD1, NKX6-1, ZNF664, MDN1, ZNF540, UBE2I, CBX5, CBX3, FOXN3, LSM5, NFKB2, KIF18A, CNOT7, DIAPH3, CPD, MYF6, LHX6, UBE2O, BRWD1, BRWD3, PICALM, HSPB9, DYRK3, KDM5D, DYRK2, YWHAB, HSPB8, FLT4, HP1BP3, CELF4, FAM208B, PIK3C2A, RBM3, ZC3H7A, SIN3A, ZNF407, POLI, RBM6, CAMK1D, ACTR6, MMP2, ETV1, TRNAU1AP, PPP2R5C, ZNF75D, SEPT2, ETV6, DUSP21, SAPCD2, TRAF6, SNURF, IRF5, LCORL, DOCK1, SSX2IP, OTUB2, NUTM1, RBM47, USP15, ZBTB43, HDAC9, AURKB, POLR2A, ZNF507, RGS20, PCBD2, HES2, PDLIM7, ZNF740, IRX2, FOXJ2, FOXJ1, TBX6, ATP2B1, WEE1, UFM1, CYP24A1, SPATA33, PITHD1, ERCC1, TAF5, NAA15, EIF3A

GO ID	Term	P-value	Genes
GO:0000784	nuclear chromosome, telomeric region	0.002760	SMCHD1, RAD51D, CBX5, HIST1H4L, CBX3, ERCC1, NHP2, HIST1H3H, THOC5, BRCA2, TERF2, HIST1H2BA
GO:0005730	nucleolus	0.021953	L3MBTL1, ZNF593, GPATCH2, GTPBP10, NOL9, GATA3, TSEN2, KLK6, OASL, FXR1, RBM3, POLR2A, SIN3A, OSBP, MDN1, FGF22, PLK4, TRMT10A, DDX18, FAM9A, CBX5, NIFK, SCAF11, DIS3, STAT1, SLC30A5, FOXJ2, PA2G4, SEPT2, ETV6, WEE1, SAPCD2, TRAF6, NHP2, TAF5, BRWD1, ERGIC2, EIF3A, YPEL2
GO:0030141	secretory granule	0.029227	CDC42, SLC30A5, AVP, BRCA2, MPO, ELANE, VAMP3
GO:0017053	transcriptional repressor complex	0.029296	CBX5, CCND1, SIN3A, YWHAB, GATA1, ELANE
GO:0005622	intracellular	0.034505	DOCK5, CHIC1, TRAF3IP2, HSPB8, PIK3C2A, TRIM8, CCND1, MCF2L, ZNF208, POLI, ZNF567, ARL5A, ZNF684, ZNF480, ATG10, SFRP1, ZNF717, ZNF93, B3GNT5, AGTR1, TRIM13, PIK3C3, ZNF677, ZNF780A, SIK2, RAPGEF5, DOCK1, GPLD1, DGKI, ZNF233, VAMP3, ZNF793, ZNF473, RAB1A, CRB1, FBLN1, AKAP5, ZNF3, ASB17, CDC42, SOCS3, ZNF701, ZNF426, ZNF227, TRIM49, ZIM2, SNX5, ZNF585A, ZNF540, CCL20, CAPN13, ZNF33A, GH1, FAT4, TRIM38
GO:0015629	actin cytoskeleton	0.044006	IVNS1ABP, SVIL, AVIL, PARVA, SRCIN1, SEPT2, PPP1R9B, SMTN, ABLIM2, STK17B, ABL2, TAF5, PDLIM7
GO:0005694	chromosome	0.048450	DDX18, SETD2, SMCHD1, C11ORF80, HP1BP3, GTPBP10, RAD1, PDS5A

Table A4. *Significantly enriched KEGG terms of DEGs.*

GO ID	Term	P-value	Genes
hsa04514	Cell adhesion molecules (CAMs)	0.018654	CLDN6, SELP, NTNG1, SDC4, CADM1, CD28, NCAM1, HLA-DOA, PVR, HLA-DQA2
hsa05416	Viral myocarditis	0.021683	CD28, FYN, HLA-DOA, BID, HLA-DQA2, ACTG1
hsa04520	Adherens junction	0.049357	SMAD2, PARD3, FYN, MET, EGFR, ACTG1
hsa04510	Focal adhesion	0.008373	COL27A1, FLT4, XIAP, PARVA, CDC42, COL3A1, CCND1, COL4A4, AKT2, COL4A6, SPP1, TNR, DOCK1, PAK2

Table A5. *Pathway enrichment analysis with ClueGO for the highest score.*

GO ID	Term	P-value	Genes
Biological process			
GO:0000288	nuclear-transcribed mRNA catabolic process, deadenylation-dependent decay	0.00	DIS3, EXOSC4, LSM5, TNRC6C
GO:1900026	positive regulation of substrate adhesion-dependent cell spreading	0.00	CDC42, NCOA3, P4HB
GO:0043486	histone exchange	0.00	CENPL, CENPU, RBBP4, TERF2
GO:0043551	regulation of phosphatidylinositol 3-kinase activity	0.01	CCR7, CDC42, SOCS3
GO:0060260	regulation of transcription initiation from RNA polymerase II promoter	0.00	ERCC1, MED4, MED6, MED8, TNRC6C
GO:0140056	organelle localization by membrane tethering	0.00	CEP70, CEP76, CEP83, CEP97, DYNC1H1, NPHP1, PLK4, TMEM67, VAMP3
GO:0007097	nuclear migration	0.00	CDC42, DYNC1H1, SUN1
GO:0070254	mucus secretion	0.00	EGFR, P2RY2, VAMP3
GO:0097746	blood vessel diameter maintenance	0.00	AGTR1, AVP, DRD1, EGFR, HTR7, P2RY2, PIK3C2A
GO:0031123	RNA 3'-end processing	0.00	CDC40, CSTF2, EXOSC4, FIP1L1, SYMPK, THOC2, THOC5
GO:1903046	meiotic cell cycle process	0.00	BRCA2, BRIP1, ERCC1, KIF18A, MRE11, RAD1, RAD51, SUN1, SYCE1
GO:0007052	mitotic spindle organization	0.00	AURKB, CENPL, CENPU, CEP97, DYNC1H1, DYNLL2, GPSM2, KIF18A, SMC1A, TPR
GO:0006312	mitotic recombination	0.00	BRCA2, ERCC1, MRE11, RAD51, TERF2
Molecular function			
GO:0008528	G protein-coupled peptide receptor activity	0.00	AGTR1, CALCR, CCR7, CXCR6, GAL, GLP1R, SCTR, TSHR
GO:0043551	regulation of phosphatidylinositol 3-kinase activity	0.01	CCR7, CDC42, SOCS3
GO:0061650	ubiquitin-like protein conjugating enzyme activity	0.00	UBE2D3, UBE2G1, UBE2I, UBE2O
GO:0004527	exonuclease activity	0.00	DIS3, EXOSC4, MRE11, RAD1, RAD9A, TERF2
Cell component			
GO:0005847	mRNA cleavage and polyadenylation specificity factor complex	0.00	CSTF2, FIP1L1, SYMPK
GO:0005868	cytoplasmic dynein complex	0.00	DYNC1H1, DYNLL2, TPR
GO:0030669	clathrin-coated endocytic vesicle membrane	0.00	AVP, EGFR, PICALM, TGOLN2, VAMP3, VAMP4
GO:0097525	spliceosomal snRNP complex	0.00	LSM5, PPIH, PRPF40A, SNRPB2
GO:0098687	chromosomal region	0.00	AURKB, BRCA2, CENPL, CENPU, ERCC1, KIF18A, MRE11, PDS5A, PPP2R5C, RAD51, SEPTIN2, SIN3A, SMC1A, TERF2, THOC2, THOC5, TPR
KEGG			

GO ID	Term	P-value	Genes
KEGG:00310	Lysine degradation	0.03	KMT2A, KMT2E, PLOD2
KEGG:03015	mRNA surveillance pathway	0.02	CSTF2, FIP1L1, PPP2R5C, SYMPK
KEGG:03040	Spliceosome	0.00	CDC40, CDC5L, LSM5, PPIH, PRPF40A, SNRPB2, THOC2
KEGG:04080	Neuroactive ligand-receptor interaction	0.00	AGTR1, AVP, CALCR, DRD1, GAL, GLP1R, GRM5, GRP, HTR7, P2RY14, P2RY2, PTGER2, PTGFR, PYY, SCTR, TSHR
KEGG:04962	Vasopressin-regulated water reabsorption	0.01	AVP, DYNC1H1, DYNLL2
KEGG:03440	Homologous recombination	0.00	BRCA2, BRIP1, MRE11, RAD51
KEGG:04974	Protein digestion and absorption	0.00	COL14A1, COL27A1, COL3A1, COL4A4, COL4A6, COL6A3

References

[1] Charlson, F. J., et al., Global Epidemiology and Burden of Schizophrenia: Findings From the Global Burden of Disease Study 2016. Schizophrenia Bulletin, 2018. 44 (6).

[2] Wolfgang Fleischhacker, W., et al., Schizophrenia—Time to Commit to Policy Change. Schizophrenia Bulletin, 2014. 40 (3): p. 165-194.

[3] Maziade, M., At Risk for Serious Mental Illness - Screening Children of Patients with Mood Disorders or Schizophre nia. N Engl J Med, 2017. 376 (10): p. 910-912.

[4] Dietz, A. G., S. A. Goldman, and M. Nedergaard, Glial cells in schizophrenia: a unified hypothesis. Lancet Psychiatry, 2020. 7 (3): p. 272-281.

[5] Bartel, D. P., Metazoan MicroRNAs. Cell, 2018. 173 (1): p. 20.

[6] Berg, M. M. J. V. D., et al., Circulating microRNAs as potential biomarkers for psychiatric and neurodegenerative disorders. Progress in Neurobiology, 2019. 185: p. 101732.

[7] Smigielski, L., et al., Epigenetic mechanisms in schizophrenia and other psychotic disorders: a systematic review of empirical human findings. Molecular Psychiatry, 2020 (11): p. 1-31.

[8] He, K., et al., Identification of serum microRNAs as diagnostic biomarkers for schizophrenia. Hereditas, 2019. 156.

[9] Lai, C. Y., et al., MicroRNA Expression Aberration as Potential Peripheral Blood Biomarkers for Schizophrenia. Plos One, 2011. 6.

[10] Ozsolak, F., et al., Chromatin structure analyses identify miRNA promoters. Genes & Development, 2008. 22 (22): p. 3172-3183.

[11] Wang, W., et al., The p53/miR-193a/EGFR feedback loop function as a driving force for non-small cell lung carcinoma tumorigenesis. Therapeutic Advances in Medical Oncology, 2019. 11.

[12] Xu, Y., et al., Exploring Transcription Factors-microRNAs Co-regulation Networks in Schizophrenia. Schizophr Bull, 2016. 42 (4): p. 1037-45.

[13] Chen, C., et al., TBtools: An Integrative Toolkit Developed for Interactive Analyses of Big Biological Data. Molecular Plant, 2020. 13 (8).

[14] Huang, D. W., et al., DAVID Bioinformatics Resources: expanded annotation database and novel algorithms to better extract biology from large gene lists. Nucleic Acids Research, 2007. 35 (suppl_2): p. W169-W175.

[15] Damian, S., et al., STRING v11: protein-protein association networks with increased coverage, supporting functional discovery in genome-wide experimental datasets. Nucleic acids research, 2018 (D1): p. D607.

[16] Ba Der, G. D. and C. Hogue, An Automated Method for Finding Molecular Complexes in Large Protein Interaction Networks. BMC Bioinformatics, 2003. 4 (1, article 2): p. 2.

[17] Gabriela, B., et al., ClueGO: a Cytoscape plug-in to decipher functionally grouped gene ontology and pathway annotation networks. Bioinformatics, 2009. 25 (8): p. 1091-1093.

[18] Bindea, G., J. Galon, and B. Mlecnik, CluePedia Cytoscape plugin: pathway insights using integrated experimental and in silico data. Bioinformatics, 2013. 29 (5): p. 661-663.

[19] Chin, C. H., et al., cytoHubba: identifying hub objects and sub-networks from complex interactome. BMC Systems Biology, 2014. 8 (S4): p. S11.

[20] Vikram, A., et al., Predicting effective microRNA target sites in mammalian mRNAs. eLife, 2015. 4: p. e05005.

[21] Georgakilas, G., et al., DIANA-miRGen v3.0: accurate characterization of microRNA promoters and their regulators. Nucleic Acids Res, 2016. 44 (D1): p. D190-5.

[22] Andlauer, T., et al., Genetic factors influencing a neurobiological substrate for psychiatric disorders. 2019.

[23] Richetto, J. and U. Meyer, Epigenetic Modifications in Schizophrenia and Related Disorders: Molecular Scars of Environmental Exposures and Source of Phenotypic Variability. Biological Psychiatry, 2020. 89 (3).

[24] Uher, R. and A. Zwicker, Etiology in psychiatry: embracing the reality of polyene-environmental causation of mental illness. World Psychiatry, 2017. 16 (2): p. 121-129.

[25] Mathoux, J., D. C. Henshall, and G. P. Brennan, Regulatory Mechanisms of the RNA Modification m6A and Significance in Brain Function in Health and Disease. Frontiers in cellular neuroscience, 2021. 15: p. 671932.

[26] Chapman, R., et al., Convergent Evidence That ZNF804A Is a Regulator of Pre-messenger RNA Processing and Gene Expression. Schizophrenia Bulletin, 2018. 45 (6255).

[27] Kanakry, C. G., et al., Neuregulin-1 regulates cell adhesion via an ErbB2/phosphoinositide-3 kinase/Akt-dependent pathway: po tential implications for schizophrenia and cancer. PLoS One, 2007. 2 (12): p. e1369.

[28] Nogami, M., et al., DGCR8-dependent efficient pri-miRNA processing of human pri-miR-9-2. Journal of Biological Chemistry.

[29] Moretti, P. N., et al., Accessing Gene Expression in Treatment-Resistant Schizophrenia. Molecular Neurobiology, 2018.

[30] Papadima, E. M., et al., Evidence towards RNA Binding Motif (RNP1, RRM) Protein 3 (RBM3) as a Potential Biomarker of Lithium Response in Bipolar Disorder Patients. Journal of Molecular Neuroence, 2017.

[31] Lelieveld, S. H., et al., Meta-analysis of 2,104 trios provides support for 10 new genes for intellectual disability. Nature Neuroscience, 2016.

[32] Bronicki, L. M. and B. J. Jasmin, Emerging complexity of the HuD/ELAVl4 gene; implications for neuronal development, function, and dysfunction. Rna-a Publication of the Rna Society, 2013. 19 (8): p. 1019-1037.

[33] Budzinska, M. I., et al., PTPN23 binds the dynein adaptor BICD1 and is required for endocytic sorting of neurotrophin receptors. Journal of Cell Science. 133 (6).

[34] Hauberg, M. E., et al., Analyzing the Role of MicroRNAs in Schizophrenia in the Context of Common Genetic Risk Variants. JAMA Psychiatry, 2016. 73 (4): p. 369-377.

[35] Kubo, M., T. Hanada, and A. Yoshimura, Suppressors of cytokine signaling and immunity. Nat Immunol, 2003. 4 (12): p. 1169-76.

[36] Ni, C., et al., LncRNA-AC006129.1 reactivates a SOCS3-mediated anti-inflammatory response through DNA methylation-mediated CIC downregulation in schizophrenia. Molecular Psychiatry, 2020.

[37] John, P. S., et al., Spatiotemporal separation of PER and CRY posttranslational regulation in the mammalian circadian clock. Proc Natl Acad Sci U S A, 2014. 111 (5): p. 2040-2045.

[38] Agapito, M. A., et al., Fetal alcohol exposure disrupts metabolic signaling in hypothalamic proopiomelanocortin neurons via a circadian mechanism in male mice. Endocrinology, 2014 (7): p. 2578-2588.

[39] Quartier, A., et al., Genes and Pathways Regulated by Androgens in Human Neural Cells, Potential Candidates for the Male Excess in Autism Spectrum Disorder. Biological Psychiatry, 2018: p. S0006322318300088.

[40] Hülskamp, G., et al., Deficiency of UBR1, a ubiquitin ligase of the N-end rule pathway, causes pancreatic dysfunction, malformations and mental retardation (Johanson-Blizzard syndrome). Nature Genetics.

[41] Florentinus-Mefailoski, A., et al., The plasma peptides of Alzheimer's disease. Clin Proteomics, 2021. 18 (1): p. 17.

[42] Li, R., et al., A Potential Autophagy-Related Competing Endogenous RNA Network and Corresponding Diagnostic Efficacy in Schizophrenia. Frontiers in Psychiatry, 2021. 12.

[43] Zhang, H. M., et al., MKL1/miR-5100/CAAP1 loop regulates autophagy and apoptosis in gastric cancer cells. Neoplasia (New York, N.Y.), 2020. 22 (5): p. 220-230.

[44] Kmioek, T., et al., The Interplay between Transcriptional Factors and MicroRNAs as an Important Factor for Th17/Treg Balance in RA Patients. International Journal of Molecular Sciences, 2020. 21 (19): p. 7169.

[45] Aja, A., et al., Further insights into the molecular complexity of the human sinus node – The role of 'novel' transcription factors and microRNAs. Progress in Biophysics and Molecular Biology, 2021.

[46] Bang-Shun, et al., Association of the DISC1 and NRG1 genetic polymorphisms with schizophrenia in a Chinese population. Gene, 2016. 590 (2): p. 293-7.

[47] Buxbaum, J. D., G. Corfas, and K. Roy, Neuregulin 1-erbB signaling and the molecular/cellular basis of schizophrenia. Nature Neuroscience, 2004. 7 (6): p. 575-580.

[48] Falls, D. L., Neuregulins: functions, forms, and signaling strategies. Experimental Cell Research, 2003. 284 (1): p. 14-30.

[49] Bertram, I., et al., Immunohistochemical evidence for impaired neuregulin-1 signaling in the prefrontal cortex in schizophrenia and in unipolar depression. Annals of the New York Academy of Sciences, 2010. 1096 (1): p. 147-156.

[50] A, V. Z. C., et al., Elevated neuregulin-1 and ErbB4 protein in the prefrontal cortex of schizophrenic patients. Schizophrenia Research, 2008. 100 (1–3): p. 270-280.